Journal of Thermal Analysis, Vol. 35 (1989) 1009–1031

Invited Review

RESULTS OF THERMAL ANALYSIS FOR INVESTIGATION OF SALT HYDRATES AS LATENT HEAT-STORAGE MATERIALS

R. Naumann and *H.-H. Emons*

BERGAKADEMIE FREIBERG, SEKTION CHEMIE
FREIBERG 9200 DDR

(Received June 17, 1988)

DTA and DSC methods and quasi-isothermal and quasi-isobaric thermogravimetry are of great importance in the investigation of salt hydrates as latent heat-storage materials. However, the transferability of the DTA and DSC results is given only for application in static latent heat-storage units. Special calorimetric methods adapted to the storage principle are preferred for the study of salt hydrates under dynamic storage conditions. The findings are discussed in connection with the examples of $Na_2SO_4 \cdot 10H_2O$, $CH_3COONa \cdot 3H_2O$, $Na_2S \cdot 9H_2O$, $Na_2S \cdot 5H_2O$, $Mg(NO_3)_2 \cdot 6H_2O$, $MgCl_2 \cdot 6H_2O$ and the eutectic mixture of $Mg(NO_3)_2 \cdot 6H_2O$–$MgCl_2 \cdot 6H_2O$.

In recent years, applications of the family of salt hydrates as latent heat-storage materials has frequently been proposed [1–3]. Latent heat-storage means utilization of the enthalpy difference of the solid–liquid or solid(I)–solid(II) phase transitions for energy storage.

At the outbreak of the first oil crisis in the early seventies, considerations concentrated on replacement of the classic heat-storage media such as water, oil and rock, the storage effect of which results from their high specific heats, by materials which produce far higher energy densities in narrow temperature ranges.

The different storage principles are shown in Table 1. The reaction heats of reversible chemical reactions are also of interest in addition to utilization of the latent heats of selected materials [8]. On separation of the reaction products following heat input, in contrast to latent heat storage, there would be a possibility for long-term heat storage, e.g. summer–winter, or the transport of heat via the transport of the components and the reverse reaction at the desired time. Unfortunately, a decisive break-through to a technical realization with regard to reaction heat storage has still not become apparent. The main difficulties are the

John Wiley & Sons, Limited, Chichester
Akadémiai Kiadó, Budapest

Table 1 Heat-storage principles

Storage principle	Material	Temperature, °C	Capacity
Sensible heat (Heat capacity)	Water	⩽ 120	4.2 MJ/m³·K
	Chamotte	⩽1000	1.5 MJ m³·K
	Grey Iron	⩽1000	4.0 MJ m³·K
	Thermooil	⩽ 250	1.9 MJ m³·K
Latent heat (Melting enthalpie)	Salthydrates	⩽ 120	200–600 MJ m³
	Salts	90–1300	150–1100 MJ/m³
	Organic compounds	⩽ 150	100–280 MJ/m³
Latent heat Lattice transformation enthalpie	Pentaerythritol	188	322 kJ/kg [5–6]
	Aminopentaerythritol	68	184 kJ/kg [4]
Reaction heat	Ammoniates	⩽1000	⩽9000 MJ/t
	Hydrogensulphates		
	Reciprocal Saltpairs		
	Metal Hydrides		
	Zeolites, Graphite-Intercalation Compounds		
	Salthydrates	⩽ 150	⩽3000 MJ/m³

control of the kinetics of the direct and reverse reactions to achieve technically interesting heat-transfer powers, and the high expense of the equipment. Developments on the dehydration of $Na_2S \cdot 5H_2O$ in the Tepidus process have been highly advanced [7, 8]. Moreover, in recent times interesting investigations of the dehydration of calcium hydroxide can be found [9].

The salt hydrates play a special part in the range of low-temperature heat for the accumulation of solar energy, the waste heat of refrigerating plants and process heat. The compounds given in the literature and shown to be promising are listed in Table 2. The melting temperatures lie between 0 and 120°. The volume-related melting enthalpy (called the storage density) normally lies between 200 and 400 MJ/m³. The highest value, 572 MJ/m³, is found in the case of $Ba(OH)_2 \cdot 8H_2O$ [10].

If the molar melting enthalpy of a salt hydrate is considered to be a function of the number of moles of bound water, there is a tendency to an increase in the energy accumulation with the content of hydrate water. The melting entropy considered by analogy shows a linear rise of 20.1 J/mol deg. Comparatively, Guion [10] found 23.1 J/mol deg. The transition from the ion lattice of the salt hydrates to the melt proceeds in a manner similar to the melting of ice, a process which is connected with an increase in entropy of 22.0 J/mol deg.

Table 2 Promising salt hydrates for application as latent heat-storage material

Salt hydrates	Melting temperature, °C	Type of melting (k = congruent) (i = incongruent)	Storage density MJ/m³
$LiClO_3 \cdot 3H_2O$	8.1	k	392.9
$NaOH \cdot 3.5H_2O$	15.4	k	284.4
$KF \cdot 4H_2O$	18.5	k	480.2
$CaCl_2 \cdot 6H_2O$	29.2	i	258.8
$Na_2SO_4 \cdot 10H_2O$	32.4	i	322.4
$Na_2CO_3 \cdot 10H_2O$	33	i	344.0
$CaBr_2 \cdot 6H_2O$	34	i	227.0
$Na_2HPO_4 \cdot 12H_2O$	35.2	i	403.2
$Zn(NO_3)_2 \cdot 6H_2O$	36	k	268.5
$KF \cdot 2H_2O$	41.4	i	316.5
$Ca(NO_3)_2 \cdot 4H_2O$	42.7	i	258.6
$Na_2S_2O_3 \cdot 5H_2O$	48	i	326.7
$Na_2HPO_4 \cdot 7H_2O$	48	i	240.0
$CH_3COONa \cdot 3H_2O$	58.4	i	364.0
$Cd(NO_3)_2 \cdot 4H_2O$	59.5	k	260.2
$NaOH \cdot H_2O$	58.0	k	467.0
$Na_2B_4O_7 \cdot 10H_2O$	68.1	i	271.0
$Na_3PO_4 \cdot 12H_2O$	69.	i	309.0
$Al(NO_3)_2 \cdot 9H_2O$	70	i	270.0
$Ba(OH)_2 \cdot 8H_2O$	78	i	572.0
$KAl(SO_4)_2 \cdot 12H_2O$	85.8	i	319.7
$Al_2(SO_4)_3 \cdot 18H_2O$	88	i	369.9
$Mg(NO_3)_2 \cdot 6H_2O$	90	k	233.0
$NH_4Al(SO_4)_2 \cdot 12H_2O$	94	k	441.0
$MgCl_2 \cdot 6H_2O$	117	i	259.0

The purely thermodynamic approach to the utilization of the melting enthalpy of the salt hydrates for heat storage has proved to be insufficient. The kinetics of the liquid–solid phase transition involves some negative phenomena which are typical of this family. The most important phenomena are:

— The tendency of the melts to subcooling.

— The phase separation of incongruently melting systems.

— A change in volume up to 13.3% ($CH_3COONa \cdot 3H_2O$).

— A low thermal conductivity of about 0.5 W/m deg compared with those of metals.

— High rates of crystallization of the subcooled melts, up to 300 cm/min in the case of $KF \cdot 4H_2O$ [11], with a tendency to crystal intergrowth.

However, the use of salt hydrates for heat storage requires the strict reversibility

of heat absorption during melting and inversely to the heat output in the course of the crystallization with the highest possible heat-transfer powers. A great number of solution of static and dynamic latent heat-storage units have been developed, mainly to overcome the irreversible phase separation phenomena [12, 13]. The static storage systems (Storage Pods, Thermol 81, STL Units [13]) are based on salt hydrates to which stabilizing agents are added. A dynamic heat-storage unit ("Galisol") variant which we have proposed comprises a four-component system consisting of salt hydrate, nucleating agent, heat-transfer liquid and tenside (Fig. 1). Heat transfer takes place by means of the vapour of the heat-transfer liquid, which is in direct contact with the salt hydrate [14–17].

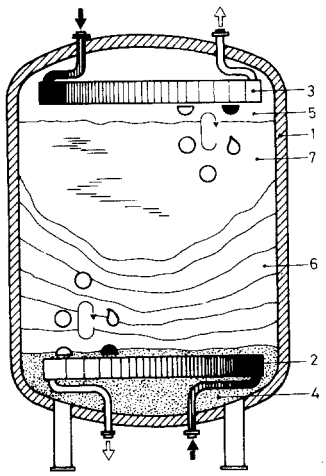

Fig. 1 Principle of "Galisol" latent heat-storage unit 1 – vessel, 2, 3 – heat exchangers, 4 – heat-transfer liquid, 5 – vapour of heat-transfer liquid, 6, 7 – salt hydrate solid, liquid

The thermoanalytical methods given below play an important part in investigations of the suitability of salt hydrates as latent heat-storage materials:

— DTA and DSC methods applied in closed sample vessels and used for determination of the melting point, melting behaviour, melting enthalpy, phase content, subcooling and stability of substance mixtures.

— Quasi-isothermal and quasi-isobaric thermogravimetry for determination of the thermal decomposition in the gas atmosphere self-generated by the sample [18].

— Technical calorimeters which allow the balancing of energy and power under heat-storage conditions.

Equilibrium methods for determination of the phases (melt–solid phase) coexisting in the solid–liquid equilibrium are of major importance, in addition to the different dynamic, quasi-isothermal and stationary thermoanalytical methods.

Investigation methods

The methods described in the following have been used by us for the investigation of salt hydrates as latent heat-storage materials:

— DTA using sample weights of about 10 mg and the DTA equipment manufactured by Setaram, France. Measuring equipment: cryostat ($-150°$ to $+500°$), crucible holder with platinel thermocouples, closed glass or Ti–Pd sample vessels.

— DTA using sample weights of about 10 g in the temperature range from $-30°$ to $+150°$ with program velocities between 0.1 and 0.5 deg/min in glass or Ti–Pd ampoules (Fig. 2). This method allows a study of the thermal behaviour of the salt hydrates under static storage conditions, and a visual observation of the phase composition.

— DSC measurements using the DSC 2 C manufactured by Perkin–Elmer, USA. The DSC measurements were carried out with the kind assistance of Dr. Flammersheim, Friedrich-Schiller-Universität Jena. The application of aluminium or steel crucibles is highly limited, due to the corrosive behaviour of many salt hydrate melts. In numerous cases, acid hydrate melts can be measured in self-made titanium–palladium crucibles.

— Calorimetric determination of the energy which can be stored in a definite temperature interval was performed in a specially adapted "Galisol" model storage unit (Fig. 3) [19, 20]. This unit works as a technical isoperibolic flow calorimeter.

The latent heat-storage material is in the vessel (1). Heat input is realized via the pipe coil (2), and heat output accordingly via (5). Water flows through the two heat exchangers, the inlet and outlet temperatures of which are recorded at the

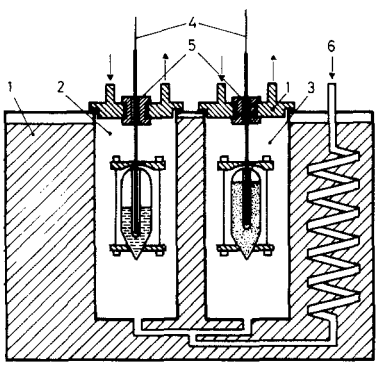

Fig. 2 DTA equipment for sample weights of about 10 g. 1 – thermostat (silicone oil), programmable, 2 – sample room with measuring ampoule, 3 – inert room with inert ampoule (α-Al_2O_3), 4 – shell thermocouple 0.5 mm (NiCr constantan) in CrNi protective tube, 5 – PTFE insulation, 6 – gas inlet—heat contact (N_2, He)

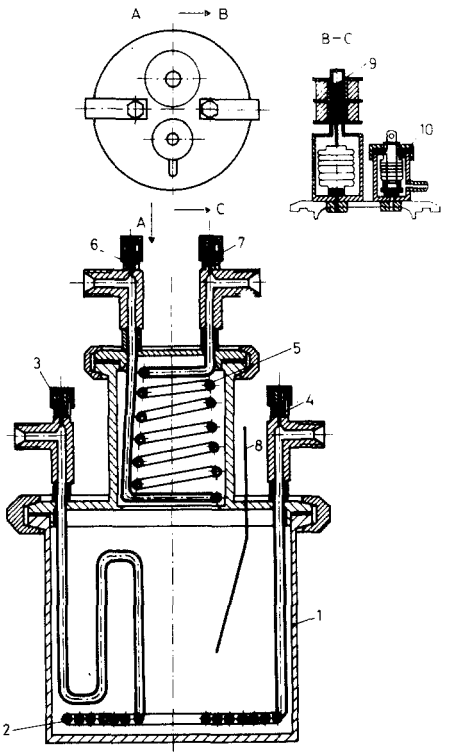

Fig. 3 Galisol latent storage unit (section drawing). 1 – storage vessel, 2,5 – heat exchangers, 3, 4, 6, 7, 8 – temperature-measuring points, 9 – inductive pressure transducer, 10 – valve

measuring points (3), (4), (6), (7). The temperature of the storage material is followed by means of the probe (8). The pressure-measuring probe with inductive transducer (9) and an outlet valve (10) are at the head of the heat-storage unit.

The heat-storage unit is coupled to thermocouples for heat charge and discharge. The water flow to the heat exchangers (2), (5) is controlled by magnetic valves. Control of the apparatus with the program cycles of heating (storing)—isothermal residence time—cooling (destoring) is carried out automatically with the output of measured values of energy, power and pressure. The theoretically storable energy Q_{th} results from the sum of the heat capacities C_{p_i} of the substance mixture and the melting enthalpy of the salt hydrate for the temperature range between ϑ_{s_2} and ϑ_{s_2} for

$$Q_{th} = \sum_{i}^{j} m_i C_{p_i} (\vartheta_{s_2} - \vartheta_{s_1}) + m_i \Delta_F H_i \qquad (1)$$

(m_i = mass; $\Delta_F H_i$ = specific melting enthalpy of component i).

The measured heat Q_{exp} results from the mass flow $\dot{m}$, the specific heat C_p and the temperature difference between the outlet and inlet of the medium which flows through the heat exchanger. In the case of water

$$Q_{exp} = \dot{m}_{H_2O} \cdot C_{pH_2O} \int_{t}^{t_2} [\vartheta_0(t) - \vartheta_y(t)]\, dt \quad (2)$$

Further instrumental details, as well as calibration for the correction of heat losses and instrument-related heat capacities, have been described in [19].

— Investigation of selected solid-liquid phase equilibria according to the isothermal agitation method, and separation of the equilibrium phases by means of a high-temperature centrifuge [21].

— Thermogravimetry according to the quasi-isothermal and quasi-isobaric method using the Q derivatograph manufactured by MOM, Hungary.

Results and discussion

$Na_2SO_4 \cdot 10H_2O$

$Na_2SO_4 \cdot 10H_2O$ (Glauber salt) is among the classic latent heat-storage materials. With its melting point of 32.4°, its melting enthalpy of 251 kJ/kg [22] and its low price, it gives most favourable conditions for low-temperature heat storage. Already in 1948, in Dover (USA) a solar power plant using Glauber salt was operated by Telkes [2]. However, after only a short time, a noticeable loss of storage capacity became apparent.

The DTA curves of $Na_2SO_4 \cdot 10H_2O$ (Fig. 4) show the irreversibility of the melting and solidification behaviour. During the first heating, water-free sodium sulphate is formed at 32.4° in the course of the incongruent melting, which precipitates on the bottom of the vessel owing to the great difference in density from that of the melt (ϱ_{melt} = 1320 kg/m³, $\varrho_{Na_2SO_2}$ = 2660 kg/m³). During cooling of the melt, two or three solidification effects are observed, which are far below the melting temperature. The observed subcooling of 20 deg (cycle 1) and 25 deg (cycles 2–4) is in good agreement with the value of 25.4 deg given in the literature [23]. The appearance of several solidification effects illustrates the incomplete rehydration of Na_2SO_4 (s) and the formation of a melt rich in water. During crystallization, this melt is converted into $Na_2SO_4 \cdot 10H_2O$, ice and repeatedly metastable $Na_2SO_4 \cdot 7H_2O$ [24, 25]. On heating, first ice melts (eutectic line at −1° [24]); $Na_2SO_4 \cdot 10H_2O$ is dissolved in the water formed until the residual amount of Glauber salt melts after the peritectic line has been reached at about 32°. Reduction of the peak face of the melting peak at 32 illustrates the decrease in melting enthalpy and, consequently, in heat capacity with the number of heating and

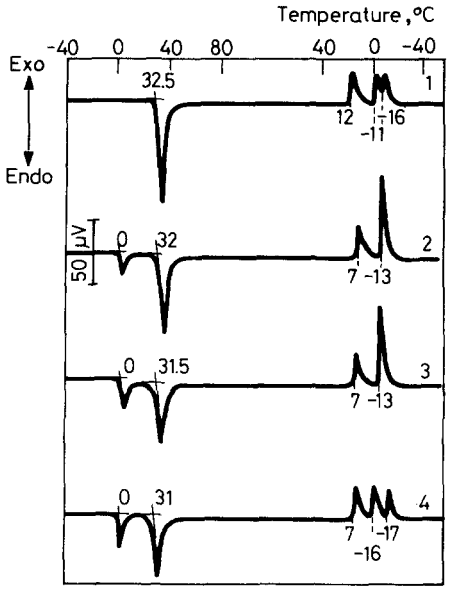

Fig. 4 DTA curves of $Na_2SO_4 \cdot 10H_2O$. $q = \pm 2$ deg/min, $m = 11.7$ mg, 1, 2, 3, 4 – cycle number

cooling cycles. The high values of subcooling emphasize the required application of $Na_2B_4O_7 \cdot 10H_2O$ as a nucleating agent for this salt hydrate [26].

In contrast with the irreversible loss of the storage capacity observed under stationary conditions, constant behaviour is noted under dynamic Galisol heat-storage conditions [19].

The results of the calorimetric evaluation of energy input and output show constant heat-storage behaviour (Fig. 5) even with high heat-transfer powers (90 ± 1 W/kg—melting, 57 ± 1 W/kg—solidification). In the temperature range 25–35°, an output of 82% of the energy calculated from the calorimetric data is found.

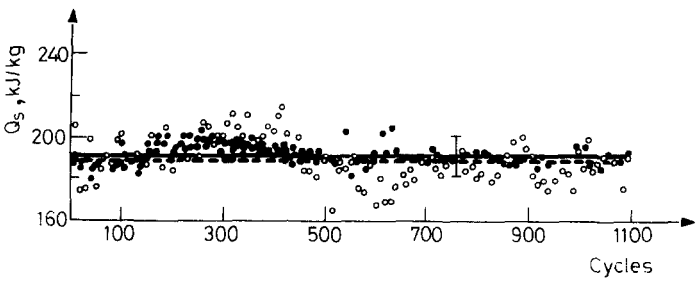

Fig. 5 Energy input and energy output of Glauber salt storage unit versus number of cycles. ○—○ input, ●—●output, $\Delta\vartheta$ = 25–35 deg

A respesentative cycle of the heat-storage unit using $Na_2SO_4 \cdot 10H_2O$ is shown in Fig. 6. It can be seen clearly that, with technically interesting heat-transfer powers involving high rates of crystallization, isothermal melting and solidification ranges (curve ϑ_s) cannot be observed. Further, the nucleation efficiency of $Na_2B_4O_7 \cdot 10H_2O$ is shown by the really low subcooling of about 1 deg in the heat output curves.

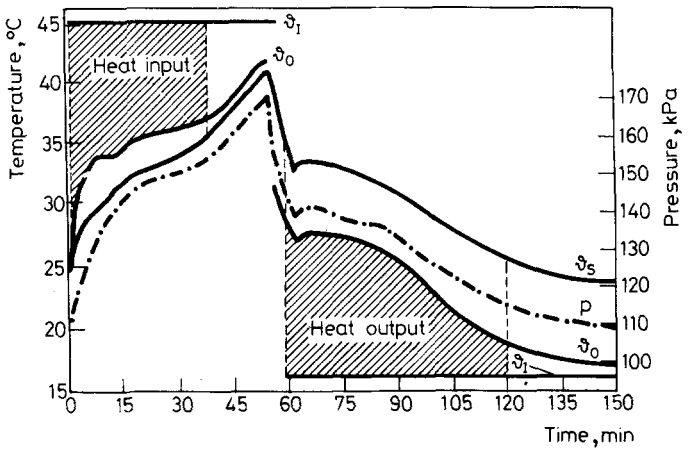

Fig. 6 Heat storage cycle of Glauber salt storage unit ϑ_i and ϑ_o—temperatures at heat exchanger inlet and outlet, respectively, ϑ_s—temperature of storage material, p—pressure

$Na_2S \cdot 9H_2O$, $Na_2S \cdot 5H_2O$

Of the hydrates of sodium sulphide, the dehydration of $Na_2S \cdot 5H_2O$ has so far been investigated for heat storage [7, 8]. The course of the dehydration in the self-generated water vapour atmosphere of 120 ± 10 kPa [27] can be followed very well via the results of quasi-equilibrium thermogravimetry. In the case of $Na_2S \cdot 9H_2O$ (Fig. 7), melting at 48° is followed by evaporation from the hydrate melt unsaturated with Na_2S. At 190°, anhydrous Na_2S is precipitated from the melt of $Na_2S \cdot 2H_2O$.

After melting at 96°, $Na_2S \cdot 5H_2O$ shows an analogous course of decomposition. Due to the higher Na_2S content in the melt, dehydration begins only at 140° (Fig. 8). The results are in good agreement with the phase diagram given by Kopylov [28].

The melting enthalpy measured via DSC is 288.9 kJ/kg for $Na_2S \cdot 9H_2O$ and 320.8 kJ/kg for $Na_2S \cdot 5H_2O$. The resulting high storage densities of 413 MJ/m³ and 486 MJ/m³ respectively, gave reason for investigation of the behaviour of these salt hydrates as latent heat-storage materials.

The results of the melting and solidification behaviour of $Na_2S \cdot 9H_2O$ are summarized in Fig. 9. On heating, the incongruent melting process begins at

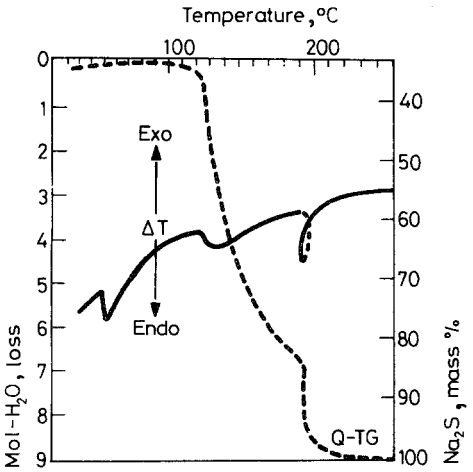

Fig. 7 Q–TG and ΔT curves of $Na_2S \cdot 9H_2O$. $m = 122.52$ mg, TG = 100 mg, $\Delta T = 250$ μV, Q–DTG = 0.6 mg/min, program II, labyrinth crucible

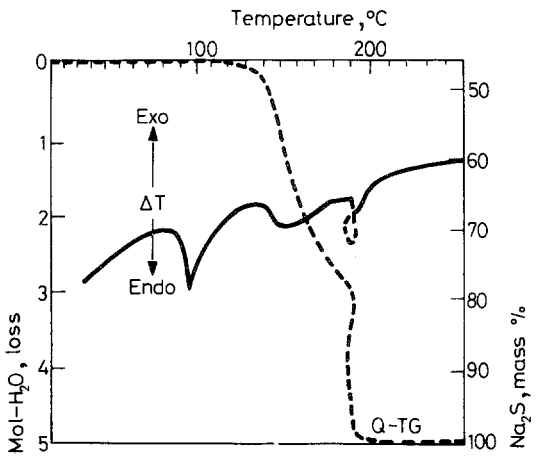

Fig. 8 Q–TG and ΔT curves of $Na_2S \cdot 5H_2O$. $m = 119.88$ mg, TG = 100 mg, $\Delta T = 250$ μV, Q–DTG = 0.6 mg/min, program II, labyrinth crucible

T_{ON} = 44–46° (small samples) or 46.5–47° (large samples) with the formation of $Na_2S \cdot 5H_2O$ (s) and melt. Dissolution of the solid phase is completed at 76°. On cooling, two or three solidification effects are observed, which result from the precipitation of $Na_2S \cdot 5H_2O$ and its conversion via the melt to $Na_2S \cdot 9H_2O$. The third peak occurring sometimes can be ascribed to small amounts of a melt rich in water, formed due to the stratification of $Na_2S \cdot 5H_2O$, with the result of the formation of ice from the melt poor in Na_2S (eutectic line at −9° [28]). A

subcooling of 38 deg is measured for small samples, but a far lower one of about 11 deg for large samples. In comparison, $Na_2S \cdot 5H_2O$ melts congruently at 96° (Fig. 10). Solidification begins at 40–57°, i.e. with a subcooling of 50–60 deg. Under static conditions, increase of the sample weight does not bring about a decrease of

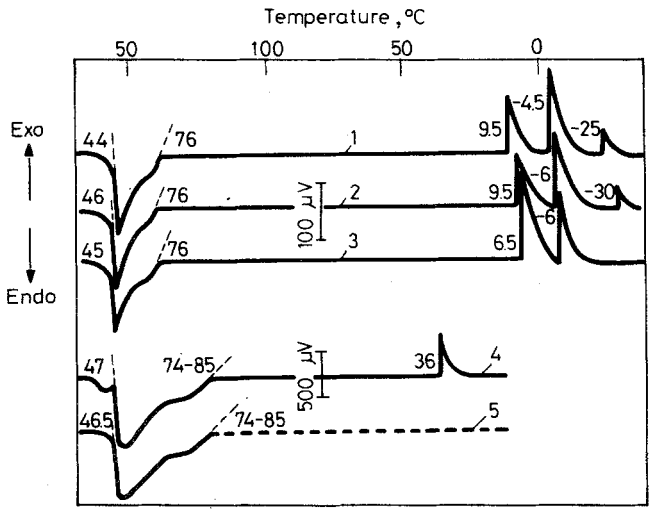

Fig. 9 Melting and solidification behaviour of $Na_2S \cdot 9H_2O$. 1–3 DTA cycles, $E = 10.915$ mg, $q = \pm 2$ deg/min. 4, 5– DTA large samples, $E = 10.75$ g, $q = \pm 0.2$ deg/min

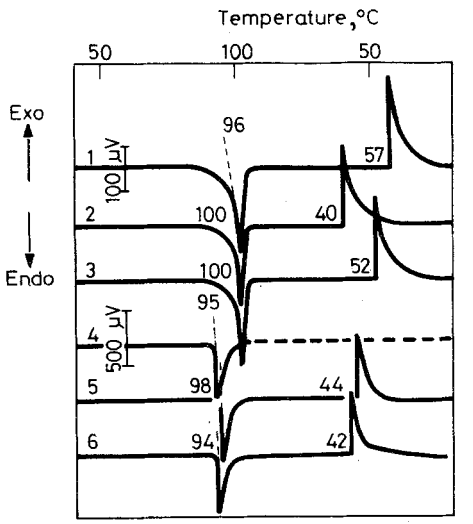

Fig. 10 Melting and solidification behaviour of $Na_2S \cdot 5H_2O$. 1–3 DTA cycles, $E = 9.256$ mg, $q = \pm 2$ deg/min, 4–6 – DTA large samples, $E = 7.341$ g, $q = \pm 0.2$ deg/min

subcooling. Suitable nucleating agents could not be found for sodium sulphide hydrate melts.

Heat-storage tests confirm the results of the DTA measurements. The distinct phase separation phenomena of $Na_2S \cdot 9H_2O$ and the high subcooling of $Na_2S \cdot 5H_2O$ did not lead to stable behaviour, even under dynamic conditions.

$CH_3COONa \cdot 3H_2O$ ($NaAc \cdot 3H_2O$)

Especially in recent years, sodium acetate trihydrate with a melting point of 58° and suitable cheapness, has again been proposed as a latent heat-storage material [29, 30]. However, high subcooling of the melts is a characteristic feature. In the DTA curve, no crystallization could be observed up to −50° (Fig. 11, curve 1). In some cases, the distinct tendency to subcooling of the melts was utilized for a specific release of heat by starting the crystallization by the addition of a crop of crystals, if required [2]. On the other hand, a great number of nucleating substances, e.g. Na_2CO_3 [31], $NaWO_4 \cdot 2H_2O$ [3], activated charcoal [32] and $Na_4P_2O_7 \cdot 10H_2O$ [33], have been proposed. A particularly large number of extensive investigations have been published into $Na_4P_2O_7 \cdot 10H_2O$ [29, 34].

The beginning of crystallization is actually already observed at 41–49° (Fig. 11, curves 2–4). If the sample weight is increased to 10 g there is a decrease in subcooling to 4.7 ± 0.3 deg in the presence of 0.5% of nucleating agent. This result is in agreement with that of Wada et al. [29], who found a subcooling of 5.3 deg. The nucleation efficiency of $Na_4P_2O_7 \cdot 10H_2O$ is lost on superheating of $NaAc \cdot 3H_2O$

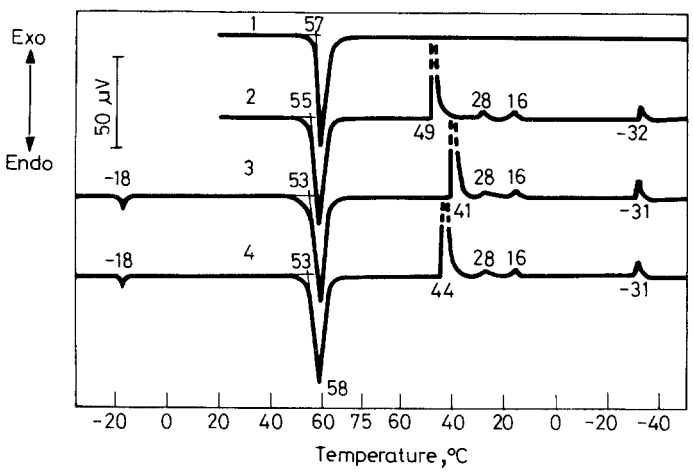

Fig. 11 DTA curves of $NaAc \cdot 3H_2O$ with an without addition of $Na_4P_2O_7 \cdot 10H_2O$. 1 – 8.3 mg $NaAc \cdot 3.27H_2O$, 2–4 – 9.0 mg $NaAc \cdot 3.27H_2O + 2.0$ mg $Na_4P_2O_7 \cdot 10H_2O$, $q = \pm 2$ deg/min

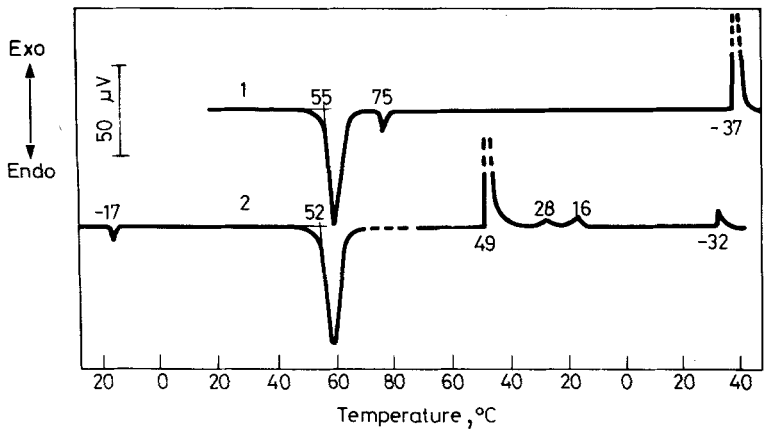

Fig. 12 DTA curves of a mixture of $NaAc \cdot 3H_2O$ ($m = 10.80$ mg) and $Na_4P_2O_7 \cdot 10H_2O$. ($m = 1.10$ mg), $q = \pm 2$ deg/min

melts or long-term heat treatment [34, 35]. In the DTA curves shown in Fig. 12, crystallization starts only at $-37°$ (Fig. 12, curve 1) after the melting of $Na_4P_2O_7 \cdot 10H_2O$ at 75° with the formation of $Na_4P_2O_7$.

The course of the solidification of $NaAc \cdot 3H_2O$ shown in Fig. 11, curves 2–4, can be observed again after the rehydration of $Na_4P_2O_7$ with the formation of $Na_4P_2O_7 \cdot 10H_2O$.

On long-term heat treatment of $NaAc \cdot 3H_2O$ melts with a solid phase of $Na_4P_2O_7 \cdot 10H_2O$, the nucleation efficiency is lost due to a solid phase transition with the formation of $Na_4P_2O_7$. Even after only 250 h at 65° and with 1 wt.% of $Na_4P_2O_7 \cdot 10H_2O$, we observed no crystallization of $NaAc \cdot 3H_2O$ melts. The transition of $Na_4P_2O_7 \cdot 10H_2O$ to $Na_4P_2O_7$ in the ternary system of $Na_4P_2O_7$–NaAc–H_2O occurs at 47° [36]. Static latent heat-storage units based on $NaAc \cdot 3H_2O$ show capacity losses. The DTA curves plotted in Fig. 11 show secondary solidification effects at 28°, 16° and $-31°$ and $-32°$. Considerable amounts of anhydrous sodium acetate are precipitated from subcooled $NaAc \cdot 3H_2O$ melts. Figure 13 shows the results of investigations of the solid–liquid phase equilibrium in the system NaAc–H_2O with the line of the metastable NaAc.

On the precipitation of NaAc, the residual melt shows a higher water content as compared with the applied $NaAc \cdot 3H_2O$. Cooling of the system below $-18°$ (eutectic line [37]) results in the formation of ice. Drying processes in the heat-storage unit can also often be a cause of trouble. The quasi-isothermal thermogravimetric results given in Fig. 14 show that a decomposition pressure of 120 ± 10 kPa is reached at 125°, and anhydrous sodium acetate is formed, which melts at $T_{ON} = 325°$.

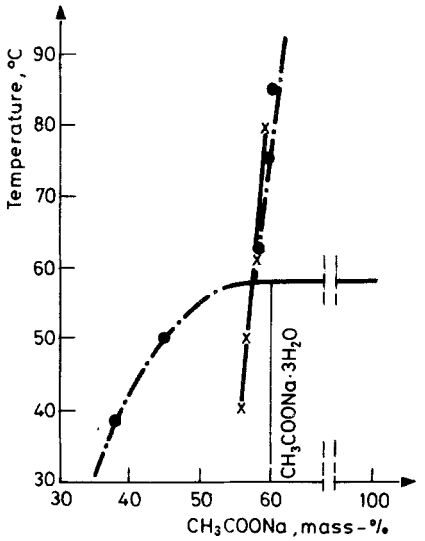

Fig. 13 Phase diagram of the system NaAc–H_2O. – · – · – [46]; · – [36]; × – present work

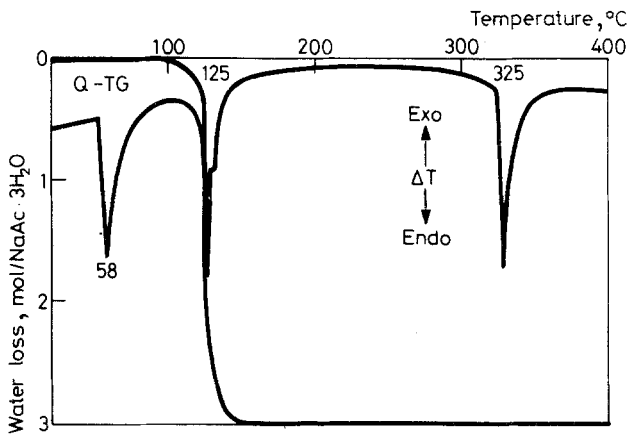

Fig. 14 Q–TG and ΔT curves of thermal decomposition of NaAc · $3H_20$. m = 187.1 mg, TG = 100 mg, ΔT = 100 μV, Q–DTG = 0.6 mg/min, program II, labyrinth crucible

In contrast with the troubling effects found under stationary conditions on application of NaAc · $3H_2O$, we observe stable storage behaviour under dynamic Galisol conditions in the presence of heat-transfer liquid and tenside. Calorimetric evaluation of 1000 cycles of heat input and heat output gave a storage capacity of 248 kJ/kg (Fig. 15) in the temperature range 50–60°, with a power of more than 50 W/kg of salt hydrate. This corresponds to a value of 84% of the theory relating

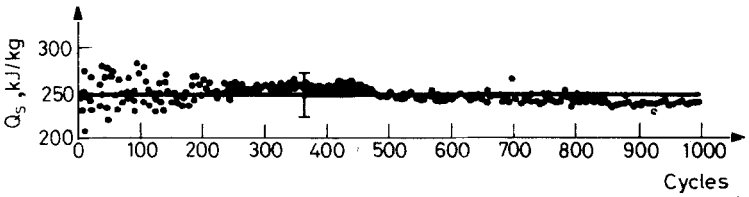

Fig. 15 Energy output of $NaAc \cdot 3H_2O$ storage unit versus number of cycles. $\Delta\vartheta$ = 50–60 deg

to the melting enthalpy of 264 kJ/kg [38] and the specific heat of 2,790 kJ/kg deg (solid) or 4,580 kJ/kg deg (liquid) [3].

$Mg(NO_3)_2 \cdot 6H_2O$

Owing to the reversibility of the melting and solidification behaviour, congruently melting compounds are to be preferred to the incongruently melting compounds. As concerns the congruently melting salt hydrates, $Mg(NO_3)_2 \cdot 6H_2O$ has frequently been proposed as a latent heat-storage material, mainly by Lane [39–41].

The DTA curves plotted in Fig. 16 show melting of the compound at 90°, and solidification with a subcooling of 30 deg (small samples) or 22.5 deg (large samples). In the solid state, there is an additional lattice transformation [25], which was found at 73° and 69.5° in the DTA plots on heating, and at 66.5° during

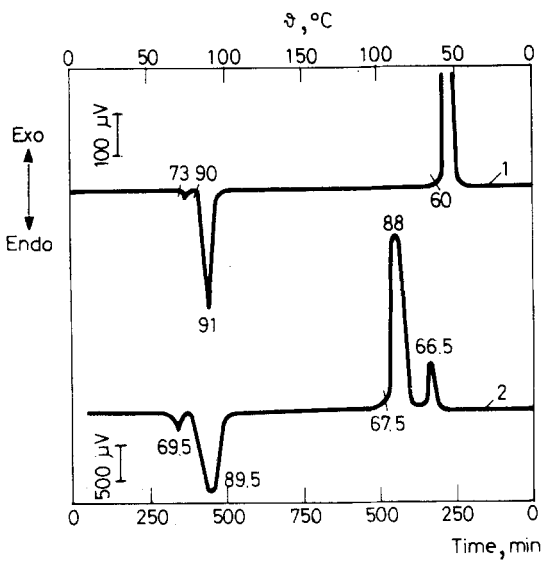

Fig. 16 DTA curves of $Mg(NO_3)_2 \cdot 6H_2O$ using different sample weights. 1 – 14.70 mg, 2 – 7.83 g

solidification. In more highly subcooled samples, the solidification effect also involves this lattice transformation. The measured enthalpy difference of 12.5 J/g agrees very well with the value of 12.1 J/g [25]. From DTA measurements under different $Mg(NO_3)_2 \cdot H_2O$ conditions, the conclusion can be drawn that this transformation occurs in the whole range of existence $Mg(NO_3)_2 \cdot 6H_2O$ (s). The results are plotted in the phase diagram in Fig. 17.

X-ray investigations have shown that there is a decrease in two space directions and an increase in the lattice parameters of the monoclinic cell in the third one [42].

For heat-storage in the range of the melting temperature, only the melting enthalpy of 150.3 J/g can be utilized.

Deviations from the stoichiometric water content lead to a clear decrease in the storable energy. The sum of the melting and transformation enthalpies of different $Mg(NO_3)_2 \cdot H_2O$ compositions in the range of stability of $Mg(NO_3)_2 \cdot 6H_2O$ is plotted in Fig. 18. Deviations of 2% compared with the stoichiometric water content lead to a 30–40 per cent reduction of the storage capacity and, of course, to a decrease in the melting temperature.

A high decrease in the melting enthalpy with deviations from the water stoichiometry was also observed in the case of the congruently melting

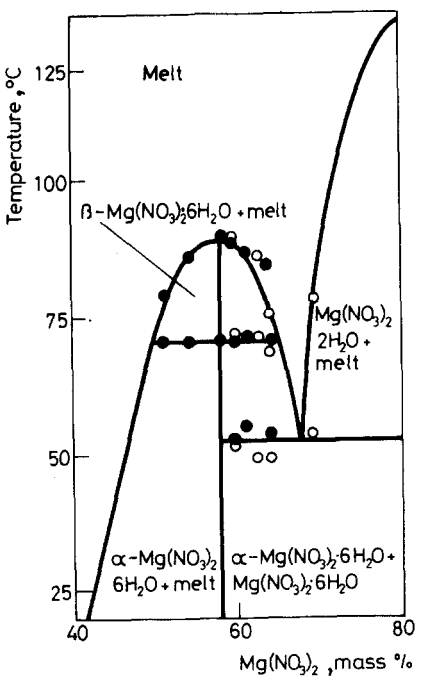

Fig. 17 Parts of phase diagram of $Mg(NO_3)_2 \cdot H_2O$ system according to [24]. ○, ●—own results [42]

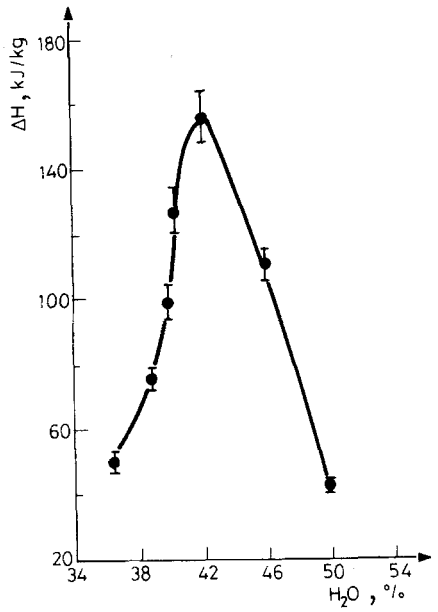

Fig. 18 Sum of melting and lattice transformation enthalpies in range of stability of β-$Mg(NO_3)_2 \cdot 6H_2O$

$NH_4Al(SO_4)_2 \cdot 12H_2O$. Moreover, a metastable form of this salthydrate having modified melting properties can be found in subcooled melts [43].

$Mg(NO_3)_2 \cdot 6H_2O$–$MgCl_2 \cdot 6H_2O$

Due to their uniform melting behaviour, eutectic mixtures of salt hydrates have frequently been proposed for latent heat storage [2, 44]. In the ternary system $Mg(NO_3)_2$–$MgCl_2$–H_2O, there exists the highest coexistence point of the hydrate phases with a high water content at 58.7 wt.% of $Mg(NO_3)_2 \cdot 6H_2O$ and 41.3% of $MgCl_2 \cdot 6H_2O$ according to Yoneda [45] at 59.1° ($\Delta_F H$ = 132.2 kJ/kg).

In the DTA curves, this eutectic point becomes apparent at an onset temperature of 63° (Fig. 19). Solidification begins at 34°. Consequently, the subcooling of the melt is 25 deg. Comparatively, Yoneda [45] gives a subcooling of 8 deg. On repeated melting, a melting effect appears reproducibly at −3°. This small amount of heat might be consumed in order to melt small quantities of α-$MgCl_2 \cdot 8H_2O$ formed during the fast solidification of the subcooled melt, to $MgCl_2 \cdot 6H_2O$ and melt. For this process, a temperature of −3.4° is given in [24].

However, the conversion of α-$MgCl_2 \cdot 8H_2O$ at low temperatures has no noticeable influence on the size and uniformity of the melting peak of the eutectic mixture, since at 59.1° only the solid phases $MgCl_2 \cdot 6H_2O$ and $Mg(NO_3)_2 \cdot 6H_2O$ are present.

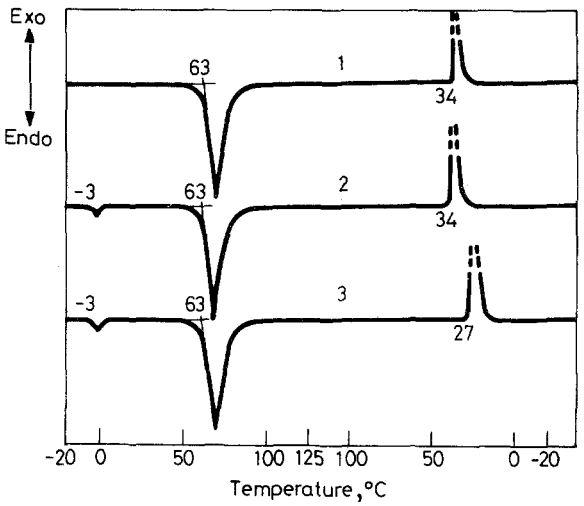

Fig. 19 DTA curves of eutectic mixture of $Mg(NO_3)_2 \cdot 6H_2O$–$MgCl_2 \cdot 6H_2O$. $m = 40.19$ mg, $q = \pm 2$ deg/min

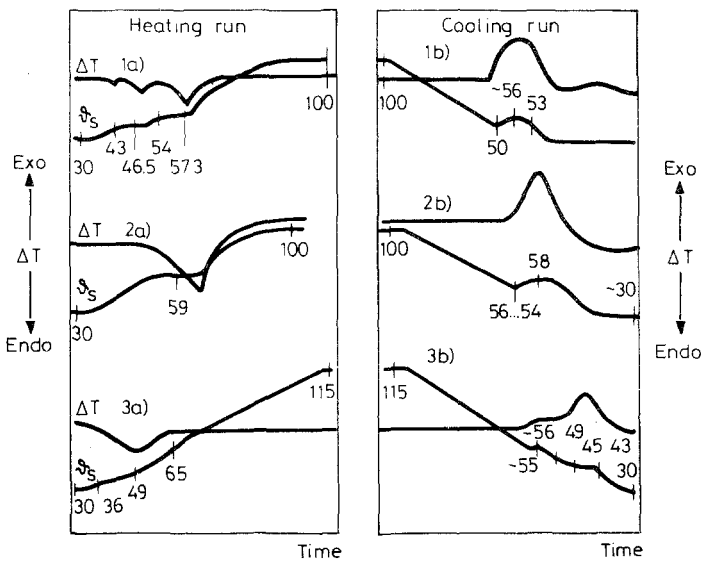

Fig. 20 DTA curves for eutectic $Mg(NO_3)_2$–$MgCl_2$ with mass ratio of 1.755 and different water contents *1a*, *1b* = 44.6% H_2O, *2a*, *2b* = 46.8% H_2O, *3a*, *3b* = 51.1% H_2O, ϑ_s = sample temperature, ΔT = temperature difference, $q = \pm 0.2$ deg/min, $m = 10$–12 g

The thermal behaviour of the system is influenced to a high degree by the water content. Figure 20 shows the DTA results at constant mass ratio with the eutectic composition $W_{Mg(NO_3)_2}/w_{MgCl_2} = 1.755$. Curves *2a* and *2b* illustrate the uniform melting and solidification behaviour. At high sample weights of 10–12 g, the subcooling reaches a maximum of only 5 deg. Even at a water deficiency of 2% (curves 1*a* and 1*b*), complicated thermal behaviour is observed, with three thermal effects. Formation of some $MgCl_2 \cdot 4H_2O$ is possible at this concentration. If there is an excess of water, thermally broad ranges of dissolution and crystallization with lower energy content can be found as compared with the eutectic composition (curves 3*a* and 3*b*).

The discussed dependence of the melting temperature and energy is also shown by the latent heat-storage behaviour (Fig. 21). The curves of heat output (●—●), beginning of solidification (○—○) and mean power (△—△) pass through a maximum, which agrees approximately with the water content (46.7%) of the eutectic mixture.

Stability investigations

The heat transfer of dynamic latent heat-storage units is frequently carried out by means of heat-transport liquids which are in direct contact with the salt hydrate. In many cases, oil [47] or halogenated hydrocarbons such as freons [48) have been proposed, owing to their chemical resistance. The thermal and chemical stabilities of less substance combinations can readily be tested by means of thermal analysis.

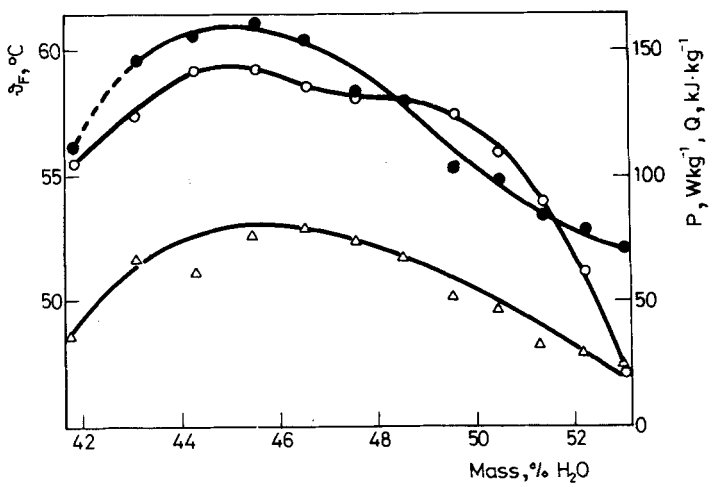

Fig. 21 Heat-storage results for the system $Mg(NO_3)_2$–$MgCl_2$–H_2O ($W_{Mg(NO_3)_2}/W_{MgCl_2} = 1.755$). ●—● Q – heat output. ○—○. ϑ_F – solidification temperature (beginning). △—△ P – mean power

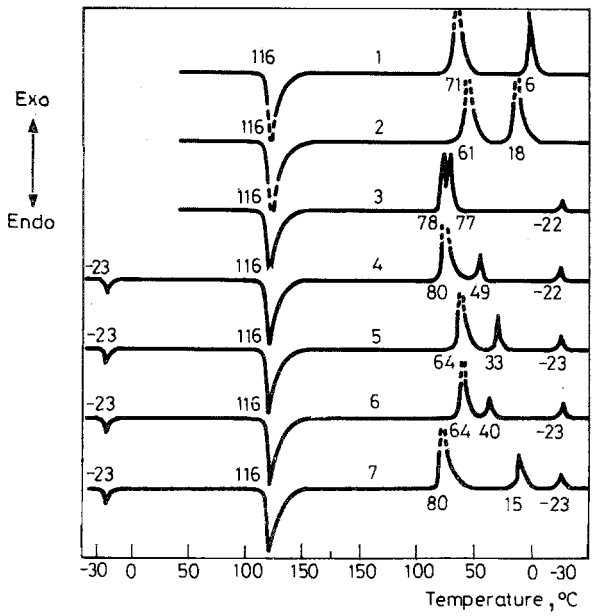

Fig. 22 DTA curves of melting and solidification behaviour of pure $MgCl_2 \cdot 6H_2O$ and its mixture with tetrachlorethene. $q = \pm 2$ deg/min, 1–2 – $MgCl_2 \cdot 6.00H_2O$, $m = 35.81$ mg, 3–6 – $MgCl_2 \cdot 6.00H_2O$, $m = 33.43$ mg, C_2Cl_4, $m = 9.00$ mg, 7 – mixture after 24 h heat treatment at 170°

This is shown in Fig. 22, on the example of $MgCl_2 \cdot 6H_2O$ in the presence of tetrachlorethene.

$MgCl_2 \cdot 6H_2O$ melts slightly incongruently at 116.7°. On solidification, in each case two exothermic effects of the crystallization of $MgCl_2$ hydrate phases (curve 1) are observed. In the presence of tetrachlorethene, the melting behaviour of $MgCl_2 \cdot 6H_2O$ remains unchanged. The crystallization peaks vary statistically in regard to their temperature. Melting and solidification peaks of tetrachlorethene additionally appear at −23° in the DTA curves (3–6) (Table: −22.4°). The thermal behaviour of the two indifferent components is preserved even after annealing of the mixture at 170° (curve 7).

Conclusions

Thermal analytical methods play an important part in investigations of the use of salt hydrates as latent heat-storage materials. For static storage units where the latent heat-storage material is in a rest position, the transferability of the results of

dynamic measuring methods of DTA and DSC in a closed system, i.e. with constant gross composition, is directly given. The frequently observed phenomenon of a decrease in subcooling of the melts, which is tantamount to an increase in the probability of nucleation, is better adapted to the conditions of application of the salt hydrates in heat-storage units, on application of high sample weights of about 10 g, with low heating rates of about 0.1 deg/min. On the basis of a great number of melting and solidification cycles over longer investigation periods, reliable statements on the behaviour of salt hydrates in heat-storage units can be made.

As concerns the behaviour of salt hydrates in dynamic heat-storage units, the methods of dynamic thermal analysis have only limited representativity. On movement of the latent heat-storage material, the velocity of the solid–liquid phase transition is increased and, consequently, reversibility is obtained. Nucleation probability under dynamic conditions is frequently very high as compared with the resting system.

Calorimetric methods specially adapted to the prevailing storage principle give the best conditions for the transferability of energy and power to the conditions in technical heat-storage units. In most cases, under the conditions of high heat-transfer powers, the concept of the isothermal storage unit operating at the melting point must be abandoned, since the required high rates of crystallization of the salt hydrates are attained only on subcooling of a few deg. The energy yields of more than 80% obtained by vapour transfer of the Galisol storage units at a temperature spread of 10 deg in the region of the melting point of the salt hydrates can be considered to be optimum.

At present, the accuracy of the thermodynamic data on most salt hydrates must be considered insufficient. The tests carried out by Guion [10] for critical inspection did not lead to any decisive breakthrough. The results are highly influenced by deviations from the stoichiometric water contents. Questions of the sample representativity play an important role. On determination of the melting enthalpies of incongruently melting compounds, the results from dynamic methods always involve solution or crystallization enthalpies of the solid phases obtained.

References

1 G. Wettermark, B. Carlson and H. Stymne, Storage of heat, a survey of efforts and possibilities, Swedish Council for Building Research to the Division of Physical Chemistry D 2: 1979.

2 G. A. Lane, Solar heat storage: Latent heat materials, Vol. I: Background and scientific principles, CRC Press Inc., Boca Raton, Florida 1983.

3 J. Schröder, Some materials and measures to store latent heat, Proc. IEA-Workshop on Latent heat stores—Technology and application, 7–9 March 1984, Institut für Kernenergetik und Energiesysteme (IKE), Universität

Stuttgart, Spezialberichte Kernforschungsanlage Jülich 1985, Nr. 297, p. 11.
4 H. G. Lorsch, K. W. Kauffmann and J. C. Denton, Energy Conversion, 15 (1975) 1.
5 T. Ozawa, Thermochim. Acta, 92 (1985) 27.
6 Y. Abe, M. Kamimoto, Y. Takahashi, R. Sakamoto, K. Kanari and T. Ozawa, Active heat exchange thermal storage unit with Pentaerythritol, Electrotechnical Laboratory, Sakura-mura, Niihari-gun, Ibaraki 305, Japan Report 849 182.
7 O. S. Dyrnum, The sodium sulphide/water system as a chemical heat pump used for long-term energy storage, Report Thermal Insulation Laboratory, Technical University of Denmark, Lyngby 1985, p. 941.
8 G. Oelert, Thermochemical heat storage, state-of-the-art report D 2: 1982, ISBN 91-540-3653-4, Swedish Council for Building Research, Stockholm, Sweden.
9 B. Lehmann, Die Pufferspeicherung thermischer Energie mittels der Wärmetönung des Systems Calciumoxid/Calciumhydroxid, Kernforschungszentrum Karlsruhe 4155, 1986.
10 J. Guion, Thermochim. Acta, 67 (1983) 167.
11 J. Schröder and K. Gawron, Energy Res., 5 (1981) 103.
12 E. van Galen, Design consideration for Latent heat stores, Proc. IEA-Workshop on Latent heat stores—Technology and application, 7–9 March 1984, Institut für Kernenergetik und Energiesysteme (IKE), Universität Stuttgart, Spezialberichte Kernforschungsanlage Jülich 1985, Nr. 297, p. 24.
13 H. Hedman, Energy Techn., 1 (1986) 10.
14 DD-PS 207758; 225857; 236862.
15 DE-OS 3324943.
16 H.-H. Emons, R. Naumann, W. Voigt, W. Stocklöw and W. Ahrens, Energy Res., 10 (1986) 69.
17 H.-H. Emons, Ö Chem Z, 12 (1987) 274.
18 J. Paulik and F. Paulik, in G. Svehla (Ed.), Analytical Chemistry, Vol. XII, Part A, Elsevier, Amsterdam 1981.
19 H.-H. Emons, R. Naumann, Th. Fanghänel and W. Ahrens, Energy Res., 13 (1989) 39.
20 DD GO 1 K/2892154.
21 W. Voigt, Th. Fanghänel and H.-H. Emons, Z. Phys. Chem., Leipzig 266, 3 (1985) 522.
22 S. Furbo and S. Svedsen, Report on heat storage in a solar heating system using salt hydrates, Thermal insulation laboratory, Technical University of Denmark, July 1977, revised February 1978.
23 J. P. Elder, Thermochim. Acta, 36 (1980) 67.
24 A. N. Kirginzev, L. N. Trushnikova and V. G. Lavrenteva, Rastvorimost neorganiceskich vesestv v vode, Isdatelstvo Chimia 1972, p. 105.
25 S. Cantor, Thermochim. Acta, 33 (1979) 69.
26 M. Telkes, Ind. and Eng. Chem., 44, 6 (1952) 1308.
27 H.-H. Emons, T. Pohl, R. Naumann and H. Voigt, Thermische Analysenverfahren in Industrie und Forschung 3, Friedrich-Schiller-Universität Jena, p. 65.
28 N. I. Kopylov, Z. Neorg. Chim. (1968) 529.
29 T. Wada, R. Yamamoto, Bull. Chem. Soc. Jap., 55 (1982) 3603.
30 JP 82 102982, 8240583, 47192.
31 L. Christensen, G. Keyser, E. Wedum, N. Cho, D. Lamb and J. Hallet, Studies of nucleation and growth of hydrate crystals with application to thermal storage systems, Desert Research Institute, Reno, Nevada, 1975.
32 Z. Stunic, V. Djurickovic and Z. Stunic, J. Appl. Chem. Biotechnol., 28 (1978) 761.
33 EP-PS 49092.
34 T. Wada, K. Matsunaga and Y. Matsuo, Bull. Chem. Soc. Jap., 57 (1984) 557.
35 R. Naumann, Th. Fanghänel and H.-H. Emons, J. Thermal Anal., 33 (1988) 685.
36 T. Wada, F. Yukotani and Y. Matsuo, Bull. Chem. Soc. Jap., 57 (1984) 1671.
37 A. Seidell, Solubility of inorganic and metalorganic compounds, 4 ed. by the American Chemical Society, Washington D.C. (1965), Vol. II, p. 854.
38 A. Pebler, Thermochim. Acta, 13 (1975) 109.
39 G. A. Lane, Int. J. of Ambient Energy, 1(3) (1980) 155.
40 US 4271029.
41 Eu 0029504.

42 R. Naumann, H.-H. Emons, F. Paulik and J. Paulik, J. Thermal Anal., 34 (1988) 1327.
43 H.-H. Emons, R. Naumann and K. Heide, Z. Anorg. Allgem. Chem., (in press).
44 H. G. Lorsch, K. W. Kauffmann and J. C. Denton, Energy Conversion, 15 (1975) 1.
45 N. Yoneda and S. Takanashi, Solar Energy, 21 (1978) 61.
46 W. F. Green, J. Phys. Chem., 12 (1908) 655.
47 F. Lindner and K. Scheunemann, Die Entwicklung eines dynamischen Glaubersalz-Latentwärmespeichers bis zur Serienreife, Report Deutsche Forschungs- und Versuchsanstalt für Luft- und Raumfahrt, DFVLR–FB 81–32.
48 EP–PS 79452.

Zusammenfassung — Bei der Untersuchung von Salzhydraten als Latentwärmespeichermaterialien besitzen DTA-, DSC-Methoden und die quasi-isotherme und quasi-isobare Thermogravimetrie eine wesentliche Bedeutung. Die Übertragbarkeit der DTA- und DSC-Ergebnisse ist jedoch nur für den Einsatz in statischen latentwärmespeichern gegeben. Für das Studium der Salzhydrate under dynamischen Speicherbedingungen werden spezielle, dem Speicherprinzip angepaßte kalorimetrische Methoden bevorzugt. Die Aussagen werden an den Beispielen $Na_2SO_4 \cdot 10H_2O$, $CH_3COONa \cdot 3H_2O$, $Na_2S \cdot 9H_2O$, $Na_2S \cdot 5H_2O$, $Mg(NO_3)_2 \cdot 6H_2O$, $MgCl_2 \cdot 6H_2O$ und der eutektischen Mischung von $Mg(NO_3)_2 \cdot 6H_2O$–$MgCl_2 \cdot 6H_2O$ diskutiert.

Резюме — Методы ДТА, ДСК и квазиизотермическая и квазиизобарная термогравиметрия являются важными методами в исследовании гидратированных солей как скрытых аккумуляторов тепла. Однако, взаимозаменяемость результатов ДТА и ДСК приведена только для применения в статических условиях. Специальные калориметрические методы адаптированные к принципу накопления, предпочтительны для изучения гидратов солей в условиях динамического накопления. Полученные данные обсуждены на примерах солей $Na_2SO_4 \cdot 10H_2O$, $CH_3COONa \cdot 3H_2O$, $Na_2S \cdot 5H_2O$, $Na_2S \cdot 9H_2O$, $Mg(NO_3)_2 \cdot 6H_2O$, $MgCl_2 \cdot 6H_2O$ и эвтектической смеси $Mg(NO_3)_2 \cdot 6H_2O$–$MgCl_2 \cdot 6H_2O$.